A&A 400, 891–902 (2003)
DOI: 10.1051/0004-6361:20021903

Astronomy & Astrophysics

Brown dwarfs in the Pleiades cluster: Clues to the substellar mass function⋆,⋆⋆

E. Moraux[1], J. Bouvier[1], J. R. Stauffer[2], and J.-C. Cuillandre[3,4]

[1] Laboratoire d'Astrophysique, Observatoire de Grenoble, BP 53, 38041 Grenoble Cedex 9, France
[2] SIRTF Science Center, California Institute of Technology, Pasadena, CA 91125, USA
[3] Canada-France-Hawaii Telescope Corp., Kamuela, HI 96743, USA
[4] Observatoire de Paris, 61 Av. de l'Observatoire, 75014 Paris, France

Received 4 November 2002 / Accepted 19 December 2002

Abstract. We present the results of a 6.4 square degrees imaging survey of the Pleiades cluster in the I and Z-bands. The survey extends up to 3 degrees from the cluster center and is 90% complete down to $I \simeq 22$. It covers a mass range from 0.03 $M_\odot$ to 0.48 $M_\odot$ and yields 40 brown dwarf candidates (BDCs) of which 29 are new. The spatial distribution of BDCs is fitted by a King profile in order to estimate the cluster substellar core radius. The Pleiades mass function is then derived accross the stellar-substellar boundary and we find that, between 0.03 $M_\odot$ and 0.48 $M_\odot$, it is well represented by a single power-law, $\mathrm{d}N/\mathrm{d}M \propto M^{-\alpha}$, with an index $\alpha = 0.60 \pm 0.11$. Over a larger mass domain, however, from 0.03 $M_\odot$ to 10 $M_\odot$, the mass function is better fitted by a log-normal function. We estimate that brown dwarfs represent about 25% of the cluster population which nevertheless makes up less than 1.5% of the cluster mass. The early dynamical evolution of the cluster appears to have had little effect on its present mass distribution at an age of 120 Myr. Comparison between the Pleiades mass function and the Galactic field mass function suggests that apparent differences may be mostly due to unresolved binary systems.

Key words. stars: low-mass, brown dwarfs – stars: luminosity function, mass function – open clusters and associations: individual: Pleiades

1. Introduction

The Initial Mass Function (IMF), i.e. the mass spectrum resulting from complex physical processes at work during star formation, is a formidable constraint for star formation models. Its determination at low stellar and substellar masses is therefore one of the main motivations for the rapidly expanding quest for brown dwarfs. Very low mass stars and brown dwarfs are also prime candidates to investigate the structure and dynamical evolution of large stellar systems, such as clusters. Searches for the lowest-mass isolated objects have been conducted in the galactic field, in young open clusters and in star-forming regions, brown dwarfs being brighter when younger. The identification of substellar candidates is often based on color magnitude diagrams (hereafter CMD) built from deep wide-field imaging surveys. One of the major shortcomings of this selection method is the contamination by older and more massive late-type field dwarfs which may lie in the same region of the CMD.

The Pleiades cluster (RA = $3^{\mathrm{h}}46.6^{\mathrm{m}}$, Dec = $+24°04'$) is an ideal hunting ground for substellar objects. It is relatively nearby with a distance of about 125 pc, with the apparent magnitude of massive brown dwarfs bright enough for being easily detected on intermediate-size telescopes. Its age of approximately 120 Myr (Stauffer et al. 1998; Martin et al. 1998) makes the lithium test particularly useful for identifying brown dwarfs: at this age, the lithium depletion boundary (in mass) coincides with the hydrogen burning mass limit (hereafter HBML). Also, the Pleiades is a rich cluster with about 1200 members and its galactic latitude is relatively high ($b = -23°$), which minimizes the possible confusion between members and red giants from the Galactic disk. Moreover, the cluster motion ($\mu_\alpha = +19$ mas/yr, $\mu_\delta = -43$ mas/yr) is large compared to that of field stars so that cluster kinematic studies are a powerful way to recognize true members among the photometric candidates.

To date, several surveys have been conducted in this cluster. They are summarized in Table 1 in term of covered area, completeness limit and number of new brown dwarfs candidates. Only surveys with a magnitude limit larger or equal to $I \simeq 17.5$ are listed here (the HBML corresponds to $Ic = 17.8$, Stauffer et al. 1998). Starting in 1997[1], several groups reported estimates for the Pleiades mass function in the upper part of the substellar domain, often represented by a single power law $\mathrm{d}N/\mathrm{d}M \propto M^{-\alpha}$ with $0.5 \leq \alpha \leq 1.0$ (see Table 1).

While these various estimates agree within uncertaintites, the substellar samples on which they rely are still relatively

Send offprint requests to: E. Moraux,
e-mail: Estelle.Moraux@obs.ujf-grenoble.fr

⋆ Based on observations obtained at Canada-France-Hawaii Telescope.

⋆⋆ Full Table 3 is only available in electronic form at the CDS via anonymous ftp to cdsarc.u-strasbg.fr (130.79.128.5) or via http://cdsweb.u-strasbg.fr/cgi-bin/qcat?J/A+A/400/891

[1] Prior to 1997, mass function estimates were based on strongly contaminated samples of brown dwarf candidates.

Table 1. Previous imaging surveys of the Pleiades conducted for searching brown dwarfs.

Survey	Area sq. degree	Completeness limit	Nb of new BD candidates	IMF index	Mass range ($M_\odot$)
Stauffer et al. (1989)	0.25	$I \sim 17.5$	4		0.2–0.08
Simons & Becklin (1992)	0.06	$I \sim 19.5$	22		0.15–0.045
Stauffer et al. (1994)	0.4	$I \sim 17.5$	2		0.3–0.075
Williams et al. (1996)	0.11	$I \sim 19$	1		0.25–0.045
Festin (1997)	0.05	$I \sim 21.6$	0	≤ 1	0.15–0.035
Cossburn et al. (1997)	0.03	$I \sim 20$	1		0.15–0.04
Zapatero et al. (1997)	0.16	$I \sim 19.5$	9	1 ± 0.5	0.4–0.045
Festin (1998)	0.24	$I \sim 21.4$	4	≤ 1	0.25–0.035
Stauffer et al. (1998)	1.	$I \sim 18.5$	3		0.15–0.035
Bouvier et al. (1998)[a,b]	2.5	$I \sim 22$	13	0.6 ± 0.15	0.4–0.04
Zapatero-Osorio et al. (1999)[b]	1.	$I \sim 21$	41		0.08–0.035
Hambly et al. (1999)	36.	$I \sim 18.3$	6	≤ 0.7	0.6–0.06
Pinfield et al. (2000)[b]	6	$I \sim 19.6$	13		0.45–0.045
Tej et al. (2002)	7	$K \sim 15$		0.5 ± 0.2	0.5–0.055
Dobbie et al. (2002)[b,c]	1.1	$I \sim 22$	10	0.8	0.6–0.030

[a] BD candidates have been confirmed by Martín et al. (2000) and Moraux et al. (2001) and the IMF index has been revised to 0.51 ± 0.15.
[b] Jameson et al. (2002) have compiled these surveys and using new infrared data they find that the Pleiades mass function is well represented by a power law with index $\alpha = 0.41 \pm 0.08$ for $0.3\ M_\odot \geq M \geq 0.035\ M_\odot$.
[c] These authors used the results from Hodgkin & Jameson (2000) and Hambly et al. (1999) to conclude that the $\alpha = 0.8$ power law is appropriate from 0.6 $M_\odot$ down to 0.03 $M_\odot$.

small and, in some cases, not fully corrected for contamination by field dwarfs. Some surveys are also quite limited spatially, and the derived mass function may not be representative of the whole cluster. In order to put the determination of the Pleiades substellar mass function on firmer grounds, we performed a deep and large survey of the Pleiades cluster in the I and Z-band, using the CFH12K camera at the Canada-France-Hawaii telescope. The survey covers 6.4 square degrees and reaches up to 3 degrees from the cluster center. It encompasses a magnitude range $I \simeq 13.5{-}24$, which corresponds to masses from 0.025 $M_\odot$ to 0.45 $M_\odot$ at the distance and age of the Pleiades.

In Sect. 2, we describe the observations and the data reduction. Results in the stellar and substellar domains are presented in Sect. 3. Forty brown dwarf candidates are identified, 29 of which are new discoveries. We discuss contamination of the photometric samples by field stars in the stellar and substellar domains, investigate the radial distribution of substellar objects, and derive the cluster substellar mass function. In Sect. 4, we discuss the overall shape of the cluster mass function over the stellar and substellar domains, the possible consequences of early cluster dynamical evolution on its present mass function and the implications for the brown dwarf formation process. A comparison is made between the Pleiades and the Galactic field mass functions, which reveals significant differences at the low mass end, a large part of which is probably attributable to unresolved cluster binaries.

2. Observations and data reduction

The I and Z observations were made using the CFH12K mosaic camera (Cuillandre et al. 2001) at the prime focus of the Canada-France-Hawaii telescope, from December 17 to 19, 2000. The camera is equipped with an array of twelve 2048×4096 pixel CCDs with 15 μm size pixels, yielding a scale of 0.206″/pixel and a field of view of 42′×28′. The I Mould and Z filter profiles are shown in Fig. 1. We obtained images of 17 fields in the Pleiades whose coordinates are given in Table 2 and the location on the sky relative to the brightest Pleiades members shown in Fig. 2. Fields were selected in order to avoid the brightest stars which would produce reflection halos and scattered light on the detectors, i.e., a higher and non uniform background which is difficult to remove. We also avoided the southwestern region of the cluster where a small CO cloud causes relatively large extinction. The observing conditions were photometric with a I-band seeing of typically 0.5″ FWHM, but occasionally up to 1.1″ FWHM.

Short and long exposures were taken for each field in order to cover a large magnitude range. We obtained a set of four images in both I and Z filters: one 10 s exposure plus three 300 s exposures in the I-band and one of 10 s exposure plus three of 360 s exposures in the Z-band. The short exposures encompass the magnitude range $13.5 \leq I \leq 21.5$ whereas the long ones cover $17 \leq I \leq 24$. A comparison between the number of stellar like objects detected in long exposures of overlapping fields indicates that the survey is about 90% complete down to $I \simeq 22$ (see Fig. 3). Note that the completeness limit of the short exposures ($I \simeq 19.5$) is much larger than the saturation limit of the long exposures ($I \simeq 17$), so that the survey completely samples the continuous mass range from 0.03 $M_\odot$ to 0.45 $M_\odot$ in the Pleiades cluster.

2.1. Photometry

Each mosaic consists of 12 CCD images which were reduced and analysed separately. The images were overscan corrected,

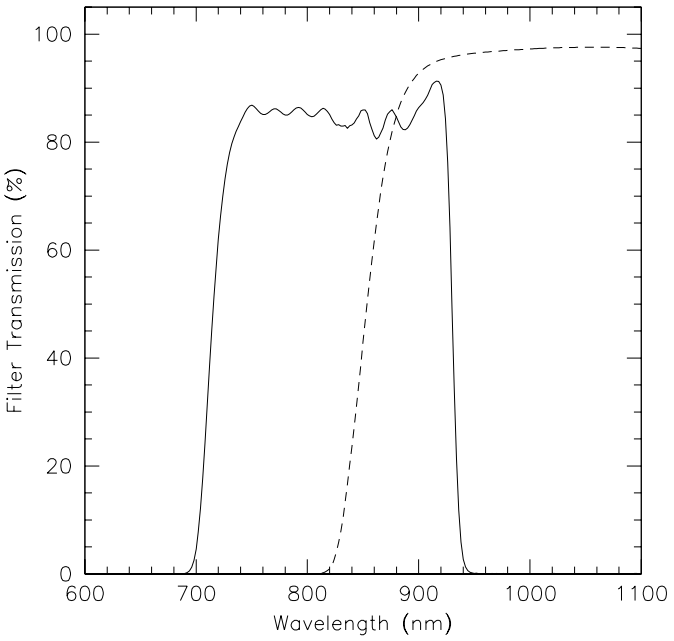

Fig. 1. Filter profiles. The solid line corresponds to the *I* Mould filter and the dashed line to the *Z* filter. The cut-off in the *Z*-band is imposed by the detector pass band.

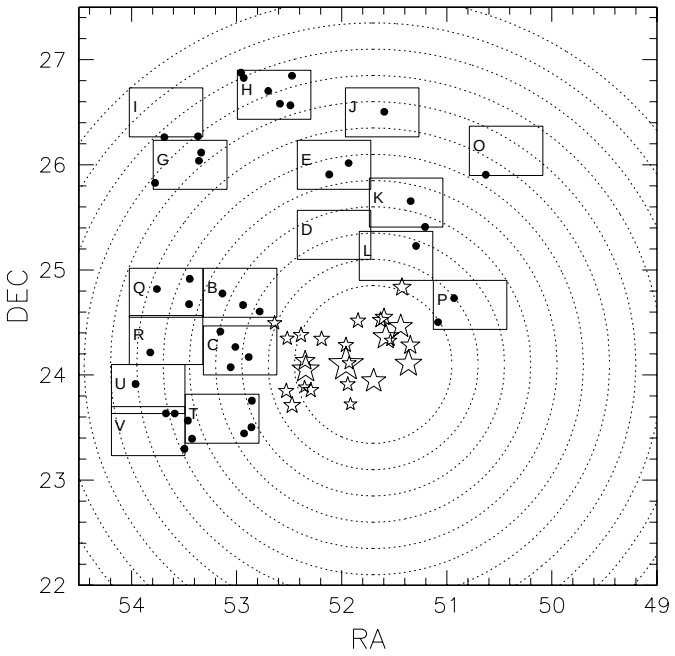

Fig. 2. Location of the 17 fields relative to the bright Pleiades members shown as stars. The size of the symbols depends on the brightness of the sources. The units are degrees on both axes. Overplotted are the circles of radii from 0.75 to 3.5 degrees centered on the cluster center. The dots represent the brown dwarf candidates detected in our survey. The total area covered by the survey amounts to 6.4 square degrees and reaches up to 3 degrees from the cluster center.

Table 2. Coordinates of the 17 different pointings observed with the CFH12K camera.

Field	RA (2000) (h m s)	Dec (2000) (° ′ ″)
Pl-B	03:51:55	24:47:00
Pl-C	03:51:55	24:14:00
Pl-D	03:48:00	25:20:00
Pl-E	03:48:00	26:00:00
Pl-G	03:54:00	26:00:00
Pl-H	03:50:30	26:40:00
Pl-I	03:55:00	26:30:00
Pl-J	03:46:00	26:30:00
Pl-K	03:45:00	25:38 30
Pl-L	03:45:25	25:08:00
Pl-O	03:40:50	26:08:00
Pl-P	03:42:20	24:40:00
Pl-Q	03:55:00	24:47:00
Pl-R	03:55:00	24:20:00
Pl-T	03:52:40	23:25:00
Pl-U	03:55:45	23:52:00
Pl-V	03:55:45	23:28:00

debiased and flat-fielded. The flats were normalized to a reference CCD to retain the appropriate relative scaling between chips. The same photometric zero-point can thus be used for all the CCDs of a mosaic. The images were also fringe-corrected using patterns derived from a smoothed combination of more than 20 images in each band. Then, images of similar exposure time for a given field were stacked together using an optimal CCD clipping to remove the artefacts, and then taking the average of the remaining final stack for each pixel to preserve the photometry.

To detect all the sources in the frames, we averaged all long exposure *I* and *Z* images of a field previously shifted to the same location and used the automatic object-finding algorithm from the Sextractor package (Bertin & Arnouts 1996). Then, a PSF-fitting photometry on the *I* and *Z* images was performed for all the detected objects using the PSFex package. We discriminated between point-like and extended or corrupted sources using the FWHM distribution of all the detected objects on each field. In practice, we defined conservative lower and upper limits around the well defined stellar peak of this distribution and rejected all the sources located outside these boundaries.

Photometric standard Landolt fields SA98 and SA113 were observed and reduced in the same way as the science images. Three successive exposures of SA98 were obtained with an incremental offset of several arcminutes in RA. Thus, common sets of photometric standard stars were observed on every CCD of the mosaic and we checked that the photometric zero-point in *I*-band was the same for each CCD: we did find a scatter of only 0.03 mag. The photometry in the *Z*-band is sensitive to detector pass band and Landolt does not give *Z* magnitudes for his standards. Thus we selected unreddened A0 standards and set their *Z* magnitude equal to their *I* magnitude assuming that their $I - Z$ color was zero (by definition of an A0 star). Thanks to the several exposures of SA98 shifted of a few arcminutes, those A0 stars were observed on different chips so that we could derive *Z* zero-points for some of the CCDs. We found a scatter of only 0.04 mag and we then used the mean value as a global zero-point, assuming that it could be used

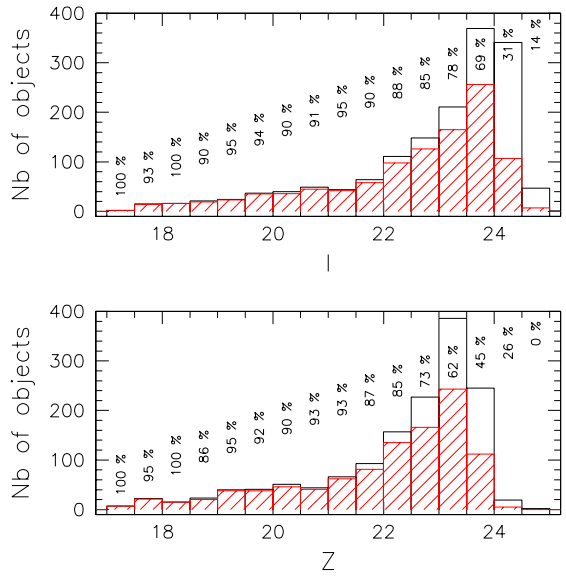

Fig. 3. The plain histograms represent the number of sources per magnitude bin I (top) or Z (bottom) detected in the field Pl-U and located in the region which overlaps with field Pl-V. Hatched histograms correspond to the number of objects detected in both fields. The percentage of matched sources is given and indicates that the survey is about 90% complete down to $I \simeq Z \simeq 22$.

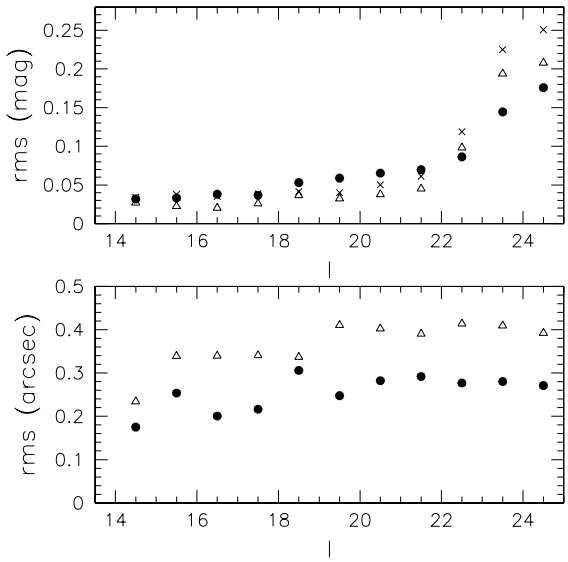

Fig. 4. *Top*: Photometric error rms plotted as a function of I magnitude. The dots correspond to the error on the magnitude I, the open triangles to the error on Z and the crosses to the error on $I - Z$; *Bottom*: Astrometric error rms shown as a function of I magnitude. The dots correspond to the error on the right ascension and the triangles denote the declination error.

for all the CCDs as in the I-band. We verified this assumption a posteriori by measuring the difference between the magnitudes of the same objects detected in the common region of 2 overlapping pointings. We thus verified that there was no systematic error and estimated the photometric rms error up to the completeness limit ($I \simeq 22$, see Fig. 4, top panel) which amounts to 0.07 mag or less at $I \leq 22$.

2.2. Astrometry

In order to obtain accurate coordinates for cluster brown dwarf candidates, we had to derive an astrometric solution for each CCD of the mosaic. We used the CFHT's Elixir package (Magnier & Cuillandre 2002) to compute the astrometric solution for each image. The algorithm calculates the celestial coordinates for all the detected objects using the approximate solution given by the header, compares them with the USNO2 catalog and refines the solution. Most of the USNO2 stars were saturated in our long exposure images so that we had to use lists of refined coordinates derived from the short exposures as a reference catalog.

We estimated the astrometric error by comparing coordinates of stars present in overlapping regions and found an accuracy better than 0.5 arcsec. The astrometric rms error is shown in Fig. 4 (bottom panel) as a function of I magnitude.

3. Results

The $(I, I - Z)$ color magnitude diagrams of the point-like objects contained in the 17 Pleiades fields are shown in Figs. 5 and 6. The short and long exposures have been analysed separately corresponding respectively to the stellar and the substellar domains. In both cases we present our photometric selection of candidates before dealing with the field star contamination. We examine the spatial distribution of cluster members and attempt to measure their core radius. We then use these estimates to derive the Pleiades mass function.

3.1. Stellar domain

The $(I, I - Z)$ color magnitude diagram for the short exposure images of our survey is presented in Fig. 5. The 120 Myr isochrone from the NEXTGEN models of Baraffe et al. (1998) shifted to the Pleiades distance ($(m - M)_o = 5.53$) is shown as a dashed line. On the basis of the location of this theoretical isochrone, we made a rather conservative photometric selection to include all possible stellar members between $I = 13.5$ and $I = 17.5$. This selection corresponds to the box drawn in Fig. 5.

To remove all the contaminating field stars from our sample, we compared our list of candidates to the results of other large Pleiades surveys. Adams et al. (2001) performed a large search for Pleiades stellar members using the photometry from the Two Micron All Sky Survey (2MASS) and proper motions determined from Palomar Observatory Sky Survey (POSS) plates. This search extends to a radius of 10° around the cluster center, well beyond the tidal radius, which means that it covers the complete cluster area. The completeness limit of the POSS plates is $I \sim 16.5$, i.e. 0.1 $M_\odot$. The authors analysed the proper motion of all the objects previously selected on the basis of their 2MASS JHK photometry and defined a membership probability p (see Adams et al. 2001 for details). We cross-correlated our list of stellar candidates with the list of all the sources analysed by Adams et al. (2001) and we kept all the objects with $p > 0.1$ so as to minimize the non-member

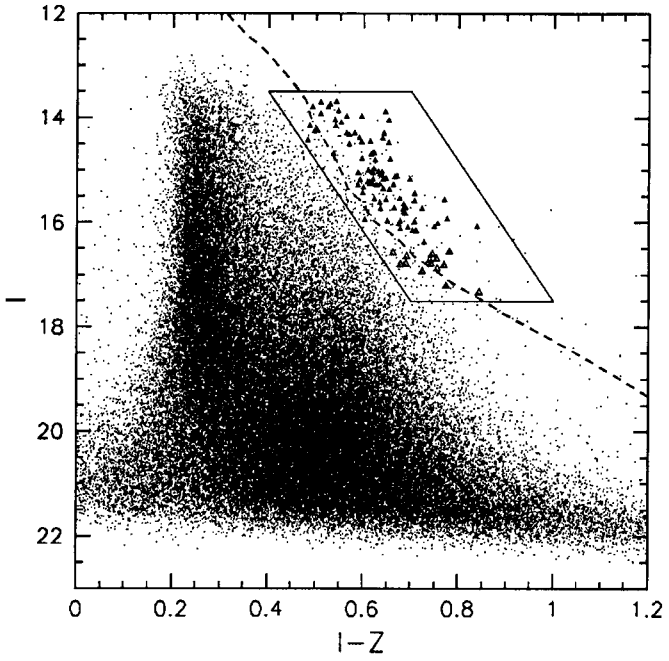

Fig. 5. $(I, I-Z)$ color-magnitude diagram for the short exposures. The dashed line is the 120 Myr isochrone from the NEXTGEN models of Baraffe et al. (1998) shifted to the Pleiades distance. The region corresponding to our photometric selection for stellar candidates corresponds to the box. Objects recovered by 2MASS and having a membership probability p based on their proper motion larger than 0.1 (Adams et al. 2001) are shown as filled triangles. Candidates too faint to be found in 2MASS but recovered by Hambly et al. (1999) and having a proper motion within 1σ of the cluster motion are indicated as open triangles.

contamination down to $I = 16.5$ (Adams' survey completeness limit). All those sources are shown as filled triangles in Fig. 5.

For stars fainter than $I > 16.5$ we compared our results with those from Hambly et al. (1999). They used photographics plates from the United Kingdom Schmidt Telescope to construct a $6^\circ \times 6^\circ$ proper motion survey centered on the Pleiades. To minimize the contamination, we chose all the objects out of our photometric candidates having proper motion within 1σ ($\simeq$20 mas/yr) of the known cluster motion ($\mu_\alpha = +19$ mas/yr, $\mu_\delta = -43$ mas/yr, Robichon et al. 1999). They are indicated as open triangles in Fig. 5.

We stopped our stellar selection at $I = 17.5$ corresponding about to Hambly's survey completeness limit but also to the HBML. A short list of those very probable low mass stellar members in our survey is presented in Table 3. We considered that the residual contamination of this sample is low enough to be neglected. The analysis of the fainter objects, i.e. substellar candidates, has been done from the long exposure images and is explained hereafter.

3.2. Substellar domain

3.2.1. Photometric selection

The $(I, I-Z)$ color magnitude of the point-like objects contained in the long exposures of the 17 Pleiades fields is shown in Fig. 6. Candidates previously identified by Bouvier et al. (1998) and confirmed on the basis of spectroscopic data, infrared photometry (Martín et al. 2000) and proper motion (Moraux et al. 2001) are shown as open circles. These objects define the high mass part of the cluster substellar sequence from $I \simeq 17.8$ down to about $I \simeq 19.5$. We note that the location of two Pleiades members (CFHT-PL-12 and CFHT-PL-16) suggest that they are likely binaries as already suspected by Bouvier et al. (1998) and Martín et al. (2000).

Table 3. Stellar candidates identified from our survey. The whole electronic list can be found on the CDS website.

No.	I	$I-Z$	RA_{J2000} (h m s)	Dec_{J2000} (° ′ ″)
1	13.69	0.54	3:51:11.55	24:23:13.30
2	13.71	0.51	3:43:09.76	24:41:32.82
3	13.75	0.53	3:51:19.05	24:10:13.08
...	...	...	...	...
111	17.21	0.77	3:52:5.82	24:17:31.16
112	17.34	0.84	3:48:50.45	25:17:54.52

We overplotted the 120 Myr isochrones from the NEXTGEN and DUSTY models from Baraffe et al. (1998) and Chabrier et al. (2000) respectively, assuming a distance modulus for the Pleiades cluster of $(m-M)_o = 5.53$, $A_V = 0.12$ and a solar metallicity. At a $T_{\rm eff}$ which corresponds to late-M and early L spectral types, dust grains begin to form, changing the opacity and resulting in objects having bluer $I-Z$ colors than predicted by the NEXTGEN models. DUSTY models instead include a treatment of dust grains in cool atmospheres for $T_{\rm eff} \leq 2300$ K. To build our sample of Pleiades brown dwarf candidates for $17.8 \leq I \leq 19$, we defined a line 0.1 mag bluer in $I-Z$ than the NEXTGEN isochrone and we selected all the sources located on the right side of this line. For $I \geq 19$, we selected all the objects redward of the DUSTY isochrone and we stopped our selection around the completeness limit, i.e. $M \simeq 0.03\ M_\odot$. All the candidates are shown in Fig. 6 as filled triangles. The photometry and coordinates of these objects are given in Table 4. Two sources are located ~0.12 mag left on the NEXTGEN isochrone at about $I = 18.5$ and have not been considered as brown dwarf candidates. The proper motion of the faintest of these two objects has been measured and indicates non-membership. The other source will be followed up but this will not change the mass function estimate.

Part of our survey overlaps with Bouvier et al.'s (1998) survey performed in 1996, so that we were able to derive proper motion for some of the objects identified in both surveys. The two epochs of observations are separated by approximately 4 years and the resulting proper motion uncertainty is typically $1\sigma \simeq 7$mas/yr. The details of the procedures used to derive proper motion are given in Moraux et al. (2001). Objects which have a proper motion less than 2σ from the cluster motion ($\mu_\alpha = +19$ mas/yr, $\mu_\delta = -43$ mas/yr) are very likely Pleiades members. We have written those objects in bold characters in Table 4 and objects whose proper motion indicates non membership in parenthesis.

Two of our new candidates had already been identified as probable Pleiades members by Pinfield et al. (2000),

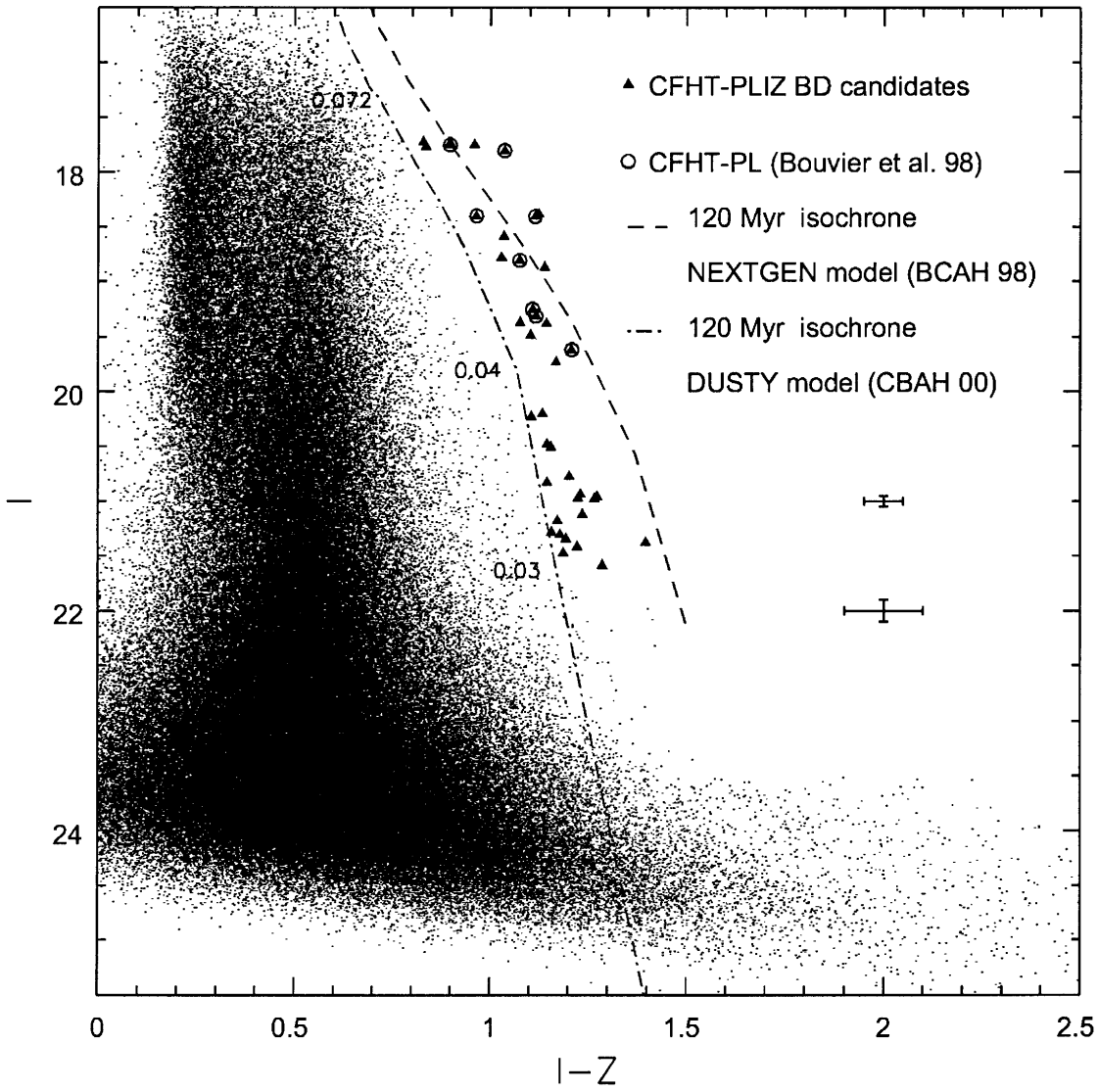

Fig. 6. $(I, I-Z)$ color magnitude diagram for the long exposures. The small dots represent the field stars. Brown dwarf candidates down to 0.03 $M_\odot$ are shown as filled triangles. Previously identified Pleiades proper motion BDs from Moraux et al. (2001) recovered by our survey are shown as open circles. The 120 Myr NEXTGEN (dashed line) and DUSTY (dot-dashed line) isochrones from Baraffe et al. (1998) and Chabrier et al. (2000) are also shown. Error bars indicate the rms photometric error.

CFHT-PLIZ-2 = BPL 327 and CFHT-PLIZ-10 = BPL 240, on the basis of their optical and infrared photometry and from their proper motion by Hambly et al. (1999). These objects are also written in bold characters in Table 4.

3.2.2. Contamination

An $(I, I-Z)$ diagram alone cannot identify objects as certain Pleiades members as one expects some level of contamination by field stars. Due to the relatively high galactic latitude of the Pleiades cluster, heavily reddened distant objects should not contaminate our photometric sample of candidate members. However, the relative location in the CMD of the theoretical Pleiades isochrone and a zero age main sequence isochrone from DUSTY models indicates that some of the photometrically selected brown dwarfs candidates could in fact be field M-dwarfs at a distance about 30% closer than the Pleiades. Considering the whole selection range which extends from 0.5 mag below the cluster sequence to the binary cluster sequence, we find that contaminating field M-dwarfs can lie in a distance range from 60 to 125 pc. Then, taking into account the area of the survey, the volume occupied by contaminants is about 1150 pc^3. The field star luminosity function for M_I = 12–14.5 can be approximated as a constant $\phi \sim 0.003$ stars/pc^3 per unit M_I as estimated from the DENIS survey (Delfosse 1997). We therefore expect to find about 7 field stars out of 21 candidates in the range I = 17.8−19.8, i.e. a contamination level of about 33% as previously derived from proper motion measurements by Moraux et al. (2001).

At fainter magnitudes the contamination level cannot be derived from the field star luminosity function which is not very well known for $M_I > 14.5$. However, we can use the number of

Table 4. Brown dwarfs candidates identified from our survey. Objects written in bold characters (resp. in parenthesis) have proper motion indicating cluster membership (resp. non cluster membership).

CFHT-PLIZ	I	$I-Z$	RA_{J2000} (h m s)	Dec_{J2000} (° ′ ″)	Other Id.
1	17.79	0.83	3:51:05.98	24:36:17.09	
2	17.81	0.90	3:55:23.07	24:49:05.01	BPL 327 (I_{KP} = 17.72), IPMBD 11 (I_C = 18.07)
3	17.82	0.90	3:52:06.72	24:16:00.76	CFHT-Pl-13 (I_C = 18.02), Teide 2 (I = 17.82), BPL 254 (I_{KP} = 17.59)
4	17.82	0.96	3:41:40.92	25:54:23.00	
5	17.84	0.84	3:53:37.96	26:02:19.67	
6	17.87	1.04	3:53:55.10	23:23:36.41	CFHT-Pl-12 (I_C = 18.00), BPL 294 (I_{KP} = 17.61)
7	18.46	1.12	3:48:12.13	25:54:28.40	
8	18.47	0.96	3:43:00.18	24:43:52.13	CFHT-Pl-17 (I_C = 18.80), BPL 49 (I_{KP} = 18.32)
9	18.47	1.11	3:44:35.19	25:13:42.34	CFHT-Pl-16 (I_C = 18.66)
10	18.66	1.03	3:51:44.97	23:26:39.47	BPL 240 (I_{KP} = 18.45)
(11)	18.85	1.03	3:44:12.67	25:24:33.62	CFHT-Pl-20 (I_C = 18.96)
12	18.88	1.07	3:51:25.61	23:45:21.16	CFHT-Pl-21 (I_C = 19.00), Calar 3 (I = 18.73), BPL 235 (I_{KP} = 18.66)
13	18.94	1.14	3:55:04.40	26:15:49.32	
14	18.94	1.14	3:53:32.39	26:07:01.20	
15	19.32	1.11	3:52:18.64	24:04:28.41	CFHT-Pl-23 (I_C = 19.33)
16	19.38	1.12	3:43:40.29	24:30:11.34	CFHT-Pl-24 (I_C = 19.50), Roque 7 (I = 19.29), BPL 62 (I_{KP} = 19.19)
17	19.44	1.08	3:51:26.69	23:30:10.65	
18	19.45	1.14	3:54:00.96	24:54:52.91	
19	19.56	1.10	3:56:16.37	23:54:51.44	
20	19.69	1.21	3:54:05.37	23:33:59.47	CFHT-Pl-25 (I_C = 19.69), BPL 303 (I_{KP} = 19.43)
21	19.80	1.17	3:55:27.66	25:49:40.72	
22	20.27	1.13	3:51:52.71	26:52:32.16	
23	20.30	1.10	3:51:33.48	24:10:14.16	
24	20.55	1.15	3:47:23.68	26:00:59.75	
(25)	20.58	1.16	3:52:44.30	24:24:50.04	
26	20.85	1.20	3:44:48.66	25:39:17.52	
(27)	20.90	1.14	3:55:00.38	23:38:08.05	
28	21.01	1.23	3:54:14.03	23:17:51.39	
29	21.03	1.27	3:49:45.29	26:50:49.88	
30	21.04	1.22	3:51:46.00	26:49:37.41	
31	21.05	1.26	3:51:47.65	24:39:59.51	
32	21.19	1.23	3:50:15.47	26:34:51.27	
33	21.25	1.17	3:50:44.68	26:42:09.36	
34	21.35	1.16	3:54:02.56	24:40:26.07	
35	21.37	1.18	3:52:39.17	24:46:30.03	
36	21.42	1.19	3:54:38.34	23:38:00.63	
37	21.45	1.40	3:55:39.57	24:12:52.12	
38	21.49	1.22	3:45:54.69	26:30:14.57	
39	21.55	1.19	3:53:40.30	26:16:18.15	
40	21.66	1.29	3:49:49.30	26:33:56.19	

stars identified in the DENIS survey down to $I = 18$ in a given color (or temperature) range in order to estimate the number of contaminants in our sample for this color interval. For example, the brown dwarf candidates with I between 20.2 and 21.7 have a temperature of ∼2000 K (Chabrier et al. 2000). We then consider the number of DENIS objects within a restricted temperature range around this value and I between 16.5 and 18, and multiply this number by two factors: a) the ratio of our CFHT survey area to the DENIS survey area, and b) the ratio of the two volumes corresponding to the two magnitude ranges (I = 20.2 to 21.7 and I = 16.5 to 18) for the DENIS survey. We thus predict 5 or 6 field dwarfs to occupy the region of the Pleiades color magnitude diagram corresponding to $0.04\ M_\odot \geq M \geq 0.03\ M_\odot$. This indicates again a contamination level of ∼30%.

For redder objects, the statistics of the DENIS survey are very low so that it is difficult to estimate the contamination. Moreover, our survey starts to be incomplete in this domain and that is why we limited our analysis to $M = 0.03\ M_\odot$.

3.3. Radial distribution

In order to deduce the total number of Pleiades members and derive the cluster mass function from a survey covering only a fraction of the cluster area, we need to investigate the spatial distribution of cluster members and its dependence on mass.

The spatial distribution of our Pleiades brown dwarf candidates is shown in Fig. 2. Overplotted are circles of radii 0.75 to 3.5 degrees centered on the cluster center. From this diagram we estimated the covered area within annulii of 0.25° width and we counted the number of substellar objects found therein. We then obtained radial surface densities for brown dwarf candidates by dividing these numbers by the corresponding surveyed areas. We proceeded in the same way for low mass stars. The number of stellar and substellar objects per square degree as a function of the radial distance is shown in Fig. 7.

The stellar distribution ($13.5 < I < 17.5$, i.e. $0.48 > M > 0.08\ M_\odot$) shown on the left panel is well fitted by a King distribution (King 1962):

$$f(x) = k\left[\frac{1}{\sqrt{1+x}} - \frac{1}{\sqrt{1+x_t}}\right]^2 \quad (1)$$

where k is a normalisation constant, $x = (r/r_c)^2$ and $x_t = (r_t/r_c)^2$ with r the radius from the cluster center. The core radius r_c increases as the stellar mass decreases and the tidal radius r_t corresponds to the location where the gravitationnal potential of the galaxy equals the cluster potential. Using $r_t = 5.54°$ from Pinfield et al. (1998), we found $k \simeq 110$ per square degrees and $r_c \simeq 2$ degrees for a median mass of our stellar sample of $M \simeq 0.2\ M_\odot$. From this radial distribution, we obtain a total of 557 stars between 0.08 and 0.48 $M_\odot$. For a dynamically relaxed cluster, the core radius is expected to vary with stellar mass as $M^{-0.5}$ and Jameson et al. (2002) derived the relationship $r_c = 0.733\ M^{-0.5}$ for the Pleiades stars. For $M \simeq 0.2\ M_\odot$, this yields $r_c \simeq 1.6°$, slightly smaller than our value.

The radial distribution of brown dwarf candidates is shown on the right side of the Fig. 7. The plain histogram corresponds to the whole list of candidates whereas the shaded histogram corresponds to objects having proper motion consistent with cluster membership (written in bold characters in Table 4). This histogram does not extend further than $r = 2.25°$ corresponding to the surveys of Pinfield et al. (2000) and Bouvier et al. (1998) from which proper motions have been derived. Those surveys were not as deep as ours so that only brown dwarf candidates brighter than $I = 20.9$ were counted. A King profile fitted to this histogram yields $r_c \simeq 1.3$ degrees as a lower limit to the cluster substellar core radius. The plain histogram also decreases in the first few radius bins but then increases further away from the cluster center. Note, however, that the uncertainties due to small number statistics are large and the plain histogram is not corrected for contamination for field stars, whose rate is expected to increase away from the cluster center. An illustrative King profile with $r_c \simeq 3.0$ degrees is shown as a possible fit to the brown dwarf distribution, mainly based on the few first radial bins. The median mass for the brown dwarfs candidates is $M \simeq 0.05\ M_\odot$ and the value expected by Jameson et al.'s (2002) relationship $r_c = 0.733\ M^{-0.5}$ is 3.4 degrees.

With $r_c \simeq 3.0°$ and $k = 28.5$ per square degrees, integration of the King distribution yields a total of ∼130 brown dwarfs between $17.8 < I < 21.7$, i.e. between 0.07 and 0.03 $M_\odot$ in the whole cluster. From this distribution, we expect to find ∼26 brown dwarfs Pleiades members in our survey out of the 40 selected candidates. This would correspond to a contamination level of 35%, quite consistent with our estimate above.

3.4. The Pleiades mass function

The Pleiades mass function can be estimated from our CFHT large survey over a continuous mass range from 0.03 $M_\odot$ to 0.45 $M_\odot$. For the stellar part (down to $I = 17.5$) we use our sample of candidates derived from short exposure images and decontaminated as explained above. We derived masses from I-band magnitudes using the 120 Myr isochrone from Baraffe et al. (1998). Below the HBML ($I \sim 17.5$) we consider our selection of brown dwarf candidates (Table 4) and we apply a correction factor of 0.7, assuming a contamination level of 30%. We used the 120 Myr isochrone from the DUSTY models of Chabrier et al. (2000) to estimate masses.

In order to correctly estimate the mass function of the whole cluster from a survey which is spatially uncomplete, one has to take into account the different radial distribution of low mass stars and brown dwarfs. Our CFHT fields are located between 0.75 and 3.5 degrees from the cluster center. We now proceed to estimate the fraction of low mass objects located in this ring compared to the total number of such objects in the cluster. For a King-profile surface density distribution, the total number of stars seen in projection within a distance r of the cluster center is obtained by integrating Eq. (1):

$$n(x) = k\pi r_c^2\left[\ln(1+x) - 4\frac{\sqrt{1+x}-1}{\sqrt{1+x_t}} + \frac{x}{1+x_t}\right]. \quad (2)$$

We consider stellar core radii following Jameson et al. (2002) relationship $r_c = 0.733\ M^{-0.5}$ and assumed a substellar core radius $r_c = 3.0°$ (see previous section). We then deduce from equation 2 that 74% of the 0.4 $M_\odot$ stars and 80% of the brown dwarfs are located within a distance from the cluster center between 0.75 and 3.5 degrees. This indicates that the relative number of brown dwarfs compared to low mass stars deduced from our survey is representative to their relative number over the whole cluster. In other words, the area covered by this survey is large enough so that any correction to the mass function for a mass-dependent radial distribution is negligeable.

The derived mass function is shown in Fig. 8 as the number of objects per unit mass. Within the uncertainties, it is reasonably well-fitted by a single power-law $\mathrm{d}N/\mathrm{d}M \propto M^{-\alpha}$ over the mass range from 0.03 $M_\odot$ to 0.45 $M_\odot$. A possibility to explain why the 0.06 $M_\odot$ data point is low is discussed in Dobbie et al. (2002). A linear regression through the data points yields an index of $\alpha = 0.60 \pm 0.11$, where the uncertainty is the 1σ fit error[2]. This result is consistent with previous estimates (cf. Table 1) and is affected by smaller uncertainties thanks to the combination of relatively large samples of low mass stars and brown dwarfs, proper correction for contamination by fields stars, and extended radial coverage of the cluster.

In Moraux et al. (2001) the mass function index was found to be $\alpha = 0.51 \pm 0.15$. Lacking a proper determination of the radial distribution of cluster members, the assumption was made that brown dwarfs and very low mass stars were similarly distributed. The index estimate was based on Bouvier et al.'s (1998) survey which covered fields spread between 0.75

[2] Using the lower limit of $r_c = 1.3°$ for the cluster core radius in the susbtellar domain would yield $\alpha = 0.63 \pm 0.11$ instead.

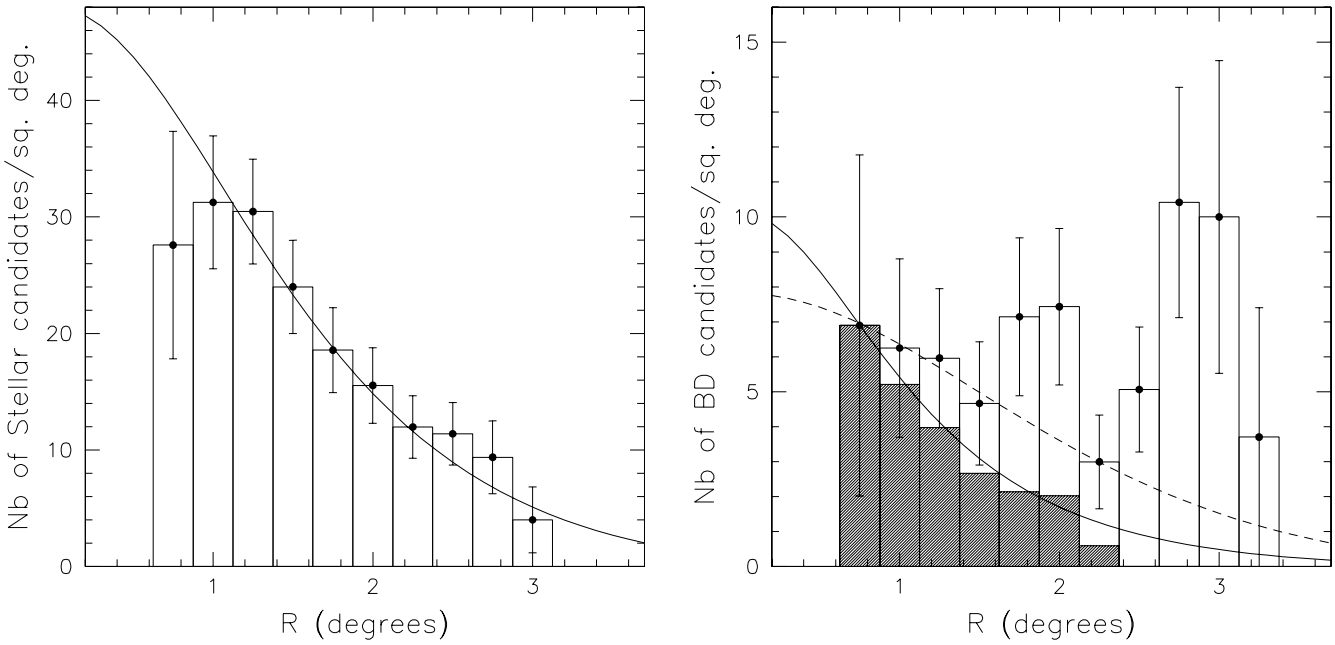

Fig. 7. *Left*: The radial distribution of probable Pleiades stellar members found in our survey and having a mass between 0.48 $M_\odot$ and 0.08 $M_\odot$ (histogram). Overplotted is the best King profile fit which, assuming $r_t = 5.54°$ (Pinfield et al. 1998), yields a core radius $r_c = 2.0°$; *Right*: The plain histogram shows the radial distribution of our brown dwarf candidates and the shaded histogram represents those which are already confirmed by proper motion. Overplotted are King profiles with $r_t = 5.54°$. The solid line is a fit of the shaded histogram which yields a lower limit of $r_c = 1.3°$ for the substellar core radius. A King profile with a core radius of $r_c = 3.0°$ is shown for reference (dashed line).

and 1.75 degrees from the cluster center. From the radial distribution derived above, we find that this annulus contains 43% of the 0.4 $M_\odot$ stars and 33% of the cluster brown dwarfs. Applying these correcting factors to the number of Pleiades members found in that survey, the mass function index becomes 0.63 instead of 0.51. This corrected value is in excellent agreement with our new estimate.

Extrapolating the power-law mass function down to $M = 0.01\ M_\odot$, we predict a total number of ~270 brown dwarfs in the Pleiades for a total mass of about 10 $M_\odot$. Clearly, while brown dwarfs are relatively numerous, they do not contribute significantly to the cluster mass. Adams et al. (2001) derived a total mass of ~800 $M_\odot$ for the Pleiades which means that, even though brown dwarfs account for about 25% of the cluster members, they represent less than 1.5% of the cluster mass.

4. Discussion

One of the main motivations for the determination of the lower mass function is to constrain the star and brown dwarf formation processes. A pressing issue is then whether the Pleiades mass function (MF) observed at an age of ~120 Myr is representative of the initial mass function (IMF), i.e. the mass spectrum resulting from the formation process.

We compare our results to the mass function of other young open clusters and star forming regions in order to investigate the dynamical evolution of the Pleiades cluster from a few Myr to its present age of 120 Myr. We also compare the Pleiades MF to the Galactic disk mass function in order to constrain the brown dwarf formation process.

4.1. Comparison to other young clusters: Clues to early dynamical evolution

We compare our results to those obtained recently for other young open clusters such as M 35 (~150 Myr, Barrado et al. in prep.) and α Per (~80 Myr, Barrado et al. 2002). The lower mass function of those clusters can be approximated by a single power-law with an index $\alpha = 0.58$ between 0.4 and 0.1 $M_\odot$ for M35 and $\alpha = 0.56$ between 0.2 and 0.06 $M_\odot$ for α Per. These values are very similar to the one determined here for the Pleiades ($\alpha = 0.60 \pm 0.11$). Results obtained for star forming regions such as σ-Orionis (~5 Myr, Bejar et al. 2001) and IC348 (~3 Myr, Tej et al. 2002) are also consistent with this value. The power-law indices are $\alpha = 0.8 \pm 0.4$ ($0.2 > M > 0.013\ M_\odot$) for σ-Orionis and $\alpha = 0.7 \pm 0.2$ ($0.5 > M > 0.035\ M_\odot$) for IC 348. The mass functions of Pleiades-age clusters and star forming regions thus appear to have a similar shape across the stellar-substellar boundary.

Comparison over a larger mass domain is best achieved by plotting the number of stars per logarithmic mass units:

$$\xi(\log M) = \frac{\mathrm{d}N}{\mathrm{d}\log M}$$

(in this representation, $\mathrm{d}N/\mathrm{d}M \propto M^{-1.0}$ corresponds to $\mathrm{d}N/\mathrm{d}\log M$ constant). Figure 9 shows the Pleiades mass function over the mass range from 0.03 $M_\odot$ to 10 $M_\odot$. The stellar portion of the mass function has been derived from the Prosser and Stauffer Open Cluster Database[3] constructed from several proper motion surveys. This catalog, however, becomes uncomplete below ~0.5 $M_\odot$. We therefore normalized our survey

[3] Available at `http://cfa-www.harvard.edu/stauffer/opencl/`

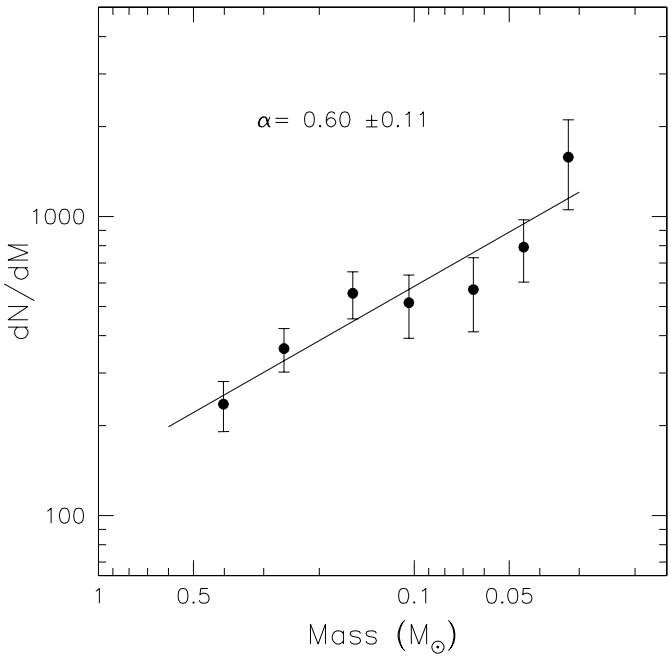

Fig. 8. The Pleiades mass function between 0.03 $M_\odot$ and 0.45 $M_\odot$. The dots corresponds to the number of objects per unit mass found in our survey. The last three points corresponds to the substellar domain and have been corrected for a 30% contamination level by field stars (see text). The data points are fitted by a power law with an index $\alpha = 0.60 \pm 0.11$ ($dN/dM \propto M^{-\alpha}$).

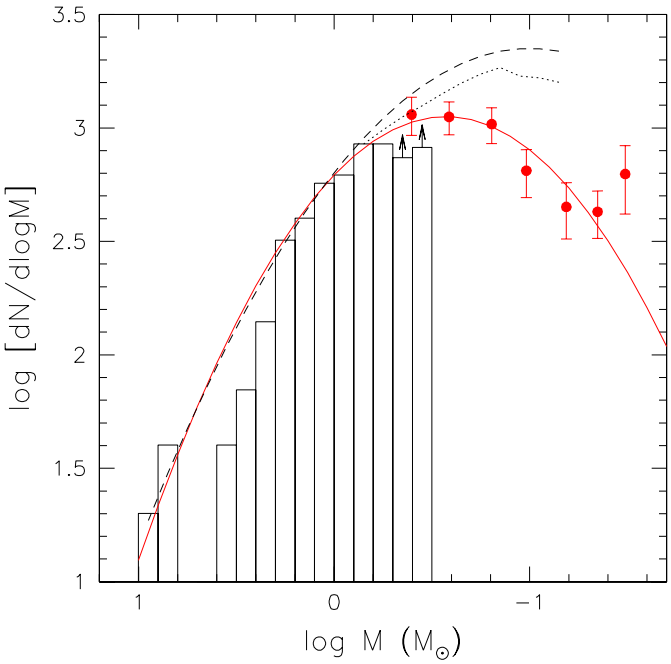

Fig. 9. The Pleiades mass function represented as the number of objects per logarithmic mass units over the mass range 0.03 $M_\odot \leq M \leq 10\ M_\odot$. In this representation Salpeter's slope is 1.35. The histogram corresponds to the Pleiades star catalog built from the Prosser and Stauffer Open Cluster Database[3] and the large dots are our data points. The Pleiades mass function is fitted by a log-normal function (solid line) over the entire mass range. The dashed line corresponds to the Galactic disk mass function from Chabrier (2001) and the dotted line to the estimated Pleiades mass function corrected for unresolved binaries.

so that the total number of objects over the 0.08–0.48 $M_\odot$ mass range corresponds to the number computed from the King profile (see Sect. 3.3). This normalization ensures the continuity of the Pleiades mass function shown in Fig. 9 from the brown dwarfs up to the most massive stars of the cluster.

The cluster mass function is fitted by a lognormal form over more than 2 decades in mass:

$$\xi(\log M) \propto \exp\left[-\frac{(\log M - \log\langle M\rangle)^2}{2\sigma^2_{\log M}}\right] \quad (3)$$

with $\langle M\rangle \simeq 0.25\ M_\odot$ and $\sigma_{\log M} = 0.52$. This mass function can be approximated by a single power-law above 1.5 $M_\odot$, $\xi(\log M) \propto M^{-1.7}$ in logarithmic mass units (or $dN/dM \propto M^{-2.7}$ in linear mass units), and peaks at $M \simeq 0.25\ M_\odot$ before decreasing at lower mass. Luhman et al. (2000) found that ρ Ophiuchus, IC 348 and the Trapezium mass functions $\xi(\log M)$ also exhibit a maximum around 0.25 $M_\odot$ and are quite similar to the Pleiades one in the stellar domain.

Within uncertainties, we thus find no evidence for significant differences in the mass function of the Pleiades, other Pleiades-age open clusters and star forming regions across the stellar-substellar boundary but also over the entire stellar domain. This suggests that the cluster population observed at an age of about 120 Myr is still quite similar to its population at only a few Myr. As a cluster evolves, weak gravitational encounters occur leading eventually to the evaporation of the lowest mass members. The results above seem to indicate that such a dynamical evolution has not yet affected the mass function of the cluster. This is in agreement with dynamical models (e.g. de la Fuente Marcos & de la Fuente Marcos 2000; Adams et al. 2002) which predict that only about 10% of the total number of cluster members is lost after ∼100 Myr, and that the fraction of brown dwarfs to stars remains nearly constant, so that the shape of the mass function across the stellar-substellar boundary is hardly affected.

The mass function of the Pleiades at an age of ∼120 Myr thus seems to be representative of the cluster population at an early age of a few Myr. But does it also reflects the initial population of the cluster at the time it formed (IMF)? Rapid dynamical processes associated to cluster formation might conceivably lead to the prompt ejection of low mass stars and brown dwarfs during the very early stage of a cluster life, before a few Myr. If instrumental, such processes might result in a depletion of the low mass cluster population very early on and thus modify the shape of the mass function.

An example of conditions under which such processes may occur is when the gas is expelled from the cluster during its formation. The gravitational potential decreases drastically and all the low mass objects in the outer part of the cluster are ejected. However, current models (Kroupa 2001) predict that roughly as many massive stars as low mass stars are ejected in this process, unless mass segregation is present initially. Hence, the shape of the mass function should not be significantly affected.

Another violent dynamical process may be associated to the formation of brown dwarfs themselves. Reipurth & Clarke (2001) proposed that substellar objects are "stellar embryos"

according to the following scenario: as molecular cloud cores fragment to form unstable protostellar multiple systems which decay dynamically, the lowest mass fragments are ejected from the core, and deprived of surrounding gas to accrete they remain substellar objects. In this scenario, the velocity dispersion may be expected to be larger for brown dwarfs than for stars and, for a fraction of substellar objects, the velocity may indeed exceed the escape velocity. Such a process could then be very efficient in quickly removing the lowest mass objects from the cluster, thus strongly modifying its initial mass function. A possibility to constrain this brown dwarf formation process would be to search for an observational signature of their primordial kinematics. Unfortunately, at an age of 120 Myr the Pleiades cluster is already largely relaxed and has lost memory of its initial evolution.

Furthermore, while several models have been developped to investigate the dynamical ejection of brown dwarfs, predictions regarding their initial velocity distribution differ. Sterzik & Durisen (1998) find that the velocity dispersion depends on both mass and binarity, being larger for low mass single objects than for massive binaries. Delgado-Donate et al. (2002) find that it depends only on binarity and that nearly all ejected objects are preferentially low mass and single ones. According to M. Bate (priv. comm.) the velocity dispersion depends neither on mass nor on binarity so that dynamical ejection of low mass objects should not affect the overall mass function of the cluster. Pending the resolution of these uncertainties, it is then difficult to assess whether the proposed ejection mechanism would lead to peculiar kinematical signatures in the substellar population and would thus possibly affect the cluster mass function. This issue is further discussed in the next section by comparing the Pleiades and the Galactic disk mass functions.

4.2. The Pleiades and Galactic disk mass functions: Clues to the brown dwarf formation process

Below ∼0.8 $M_\odot$ field stars have not had time to evolve off the main sequence, so that the observed Galactic disk mass function ought to be representative of the initial mass function. A log-normal fit to the Galactic disk mass function in the mass range 0.1–1.0 $M_\odot$ has been derived by Chabrier (2001) based on large scale photometric surveys of low mass stars in the solar neighbourhood. This log-normal approximation to the field mass function is shown as a dashed line in Fig. 9 where it has been normalized so as to have the same number of 1 $M_\odot$ stars as in the Pleiades. Major differences clearly appear between the Pleiades and the field mass functions at low masses. The log normal mass function peaks at $M \simeq 0.1\ M_\odot$ for the disk population and at $\simeq 0.25\ M_\odot$ for Pleiades members. Furthermore, Chabrier (2002) estimates that the brown dwarf population in the disk is comparable in number to the stellar one, $N_{\rm BD} \simeq N_*$, and that the substellar mass contribution to the disk budget amounts to about ∼10%. In the Pleiades, we have instead $N_{\rm BD} \simeq N_*/3$ and a brown dwarf mass contribution to the cluster mass of only 1.5%. Indeed, the Pleiades mass function lies well below the disk's one at the stellar-substellar boundary in Fig. 9.

Part of the observed difference may arise from the effect of binarity, which is not accounted for in the Pleiades mass function. While the Pleiades mass function derived above includes unresolved cluster binaries, the Galactic disk mass function has been derived for the single star population (i.e. all binaries are resolved, cf. Chabrier 2001). In order to correct the observed Pleiades mass function for unresolved binaries at low masses, we follow Luhman et al. (1998) who used a Monte Carlo technique to estimate the difference between single star and system mass functions. Assuming that the properties of field binaries derived by Duquennoy & Mayor (1991) apply to Pleiades systems (cf. Bouvier et al. 1997), we form unresolved binaries by randomly pairing objects drawn from a segmented power law mass function which represents the single star mass distribution down to the stellar-substellar boundary[4]. For an assumed 50% binary fraction in the Pleiades cluster, we find no major differences between the star and system mass functions at $M > 0.6\ M_\odot$ since above this mass the presence of a low mass companion does not significantly affect the determination of the primary's mass. Below 0.6 $M_\odot$ down to 0.07 $M_\odot$, however, we find $\Delta\alpha \sim 0.5$ between the power law exponents of the single star and system mass functions.

Then, approximating the log-normal form of the Pleiades mass function derived above by a three-segment power-law between 0.07 $M_\odot$ and 0.6 $M_\odot$, we estimate the binary corrected Pleiades mass function which is shown in Fig. 9 (dotted line). The binary corrected Pleiades mass function and the Galactic disk mass function now both peak around 0.13–0.1 $M_\odot$ and their shapes are roughly identical in the stellar domain down to 0.07 $M_\odot$. This suggests that the difference between the observed Pleiades and Galactic disk mass functions in the stellar range is merely the result of unresolved Pleiades binaries. When binarity is properly accounted for, the stellar mass function of the Pleiades is consistent with that of field stars of the solar neighbourhood. The comparison of the two mass functions in the substellar domain cannot be as detailed, due to the large uncertainties still affecting the derivation of the substellar mass function in the Galactic disk. Chabrier (2002) derives an upper limit of $\alpha \leq 1$ for a power law approximation of the field substellar mass function (see also Reid et al. 1999). This upper limit is consistent with the Pleiades substellar mass function exponent $\alpha \simeq 0.6$ derived above.

The similarity of the Pleiades and field mass functions down to at least the substellar limit and possibly below suggests that low mass objects have remained in the cluster at the time of its formation. Hence, we do not find evidence for massive ejection of the lowest mass objects early in the life of the cluster, which suggests either that dynamical ejection from protostellar groups is not the dominant mode of brown dwarf formation, or that this process yields a velocity dispersion for brown dwarfs which is not different from that of stars.

[4] We do not attempt to correct the observed Pleiades mass function for unresolved binaries in the substellar domain because the brown dwarf binary statistics is still very poorly known, as is the statistics of brown dwarfs companions to low mass stars

5. Conclusion

We have conducted a deep wide field photometric survey of the Pleiades cluster to build a sample of probable cluster members with masses in the range 0.03 $M_\odot$ to 0.48 $M_\odot$. We have identified 40 brown dwarfs candidates, of which 29 are new discoveries. Taking into account the radial distribution of cluster members, we derive the cluster mass function accross the stellar-substellar boundary. We find that a single power-law $\mathrm{d}N/\mathrm{d}M \propto M^{-\alpha}$ with an index $\alpha = 0.60 \pm 0.11$ provides a good match to the cluster mass function in the 0.03−0.48 $M_\odot$ range. This new estimate is based on a survey which combines a large radial coverage of the cluster and a realistic assessment of the contamination by field stars. Furthermore, the survey completely covers the 0.03−0.48 $M_\odot$ mass range, so that the result does not rely on the combination of heterogeneous surveys, as has been the case before. We therefore believe this new estimate is reasonably robust. Small changes may be expected when our survey will be followed up with either infrared photometry and/or proper motions.

Over a larger mass domain, covering almost 3 decades in masses from 0.03 $M_\odot$ to 10 $M_\odot$, we find that the cluster mass function is better fitted by a log-normal distribution with $\langle M \rangle \simeq 0.25\ M_\odot$ and $\sigma_{\log M} \simeq 0.52$. When unresolved Pleiades binaries are taken into account, the log-normal Pleiades mass function is not unlike the Galactic disk mass function. This suggests that the dynamical evolution of the cluster has had yet little effect on its mass content at an age of 120 Myr. It also suggests that the brown dwarf formation process does not lead to the dynamical evaporation of substellar objects at the time the cluster forms.

Acknowledgements. We thank E. Bertin for allowing us access to PSFex before public release, E. Magnier for his help in the astrometric calibration of the frames, J. Adams and N. Hambly for providing us data in electronic form prior to publication, I. Baraffe for computing specific substellar isochrones for us and K. Luhman for providing his Monte-Carlo software program to estimate the effect of unresolved binaries on the mass function. We also gratefully aknowledge helpful discussions with X. Delfosse on estimating field star contamination from DENIS data, with M. Bate, C. Clarke, E. Delgado and M. Sterzik on the dynamical evolution of young brown dwarfs in clusters, and with G. Chabrier who brought our attention on the Galactic disk mass function and on the effect unresolved binary systems might have on the shape of the observed mass function.

References

Adams, J. D., Stauffer, J. R., Monet, D. G., Skrustskie, M. F., & Beichman, C. A. 2001, AJ, 121, 2053
Adams, T., Davies, M. B., Jameson, R. F., & Scally, A. 2002, MNRAS, 333, 547
Barrado y Navascués, D., Bouvier, J., Stauffer, J. R., Lodieu, N., & McCaughrean, M. J. 2002, A&A, 395, 813
Baraffe, I., Chabrier, G., Allard, F., & Hauschildt, P. H. 1998, A&A, 337, 403
Bejar, V. J. S., Martín, E. L., Zapatero-Osorio, M. R., et al. 2001, ApJ, 556, 830
Bertin, E., & Arnouts, S. 1996, A&AS, 117, 393
Bouvier, J., Rigaut, F., & Nadeau, D. 1997, A&A, 323, 139
Bouvier, J., Stauffer, J. R., Martín, E. L., et al. 1998, A&A, 336, 490
Chabrier, G., Baraffe, I., Allard, F., & Hauschildt, P. H. 2000, ApJ, 542, 464
Chabrier, G. 2001, ApJ, 554, 1274
Chabrier, G. 2002, ApJ, 567, 304
Cuillandre, J.-C., Starr, B., Isani, S., & Lupino, G. 2001, Experimental Astronomy, 11(3), 223
Cossburn, M. R., Hodgkin, S. T., Jameson, R. F., & Pinfield, D. J. 1997, MNRAS, 288, L23
Delfosse, X. 1997, Ph.D. Thesis, Université de Grenoble
Delgado-Donate, E., Clarke, C., & Bate, M. R. 2002, MNRAS, submitted
Dobbie, P. D., Pinfield, D. J., Jameson, R. F., & Hodgkin, S. T. 2002, MNRAS, 335, L79
Dobbie, P. D., Kenyon, F., Jameson, R. F., et al. 2002, MNRAS, 335, 687
Duquennoy, A., & Mayor, M. 1991, A&A, 248, 485
Festin, L. 1997, A&A, 322, 455
Festin, L. 1998, A&A, 333, 497
de la Fuente Marcos, R., & de la Fuente Marcos, C. 2000, Ap&SS, 271, 127
Hambly, N. C., Hawkins, M. R. S., & Jameson, R. F. 1993, A&AS, 100, 607
Hambly, N. C., Hodgkin, S. T., Cossburn, M. R., & Jameson, R. F. 1999, MNRAS, 303, 835
Hodgkin, S. T., & Jameson, R. F. 2000, Stellar Clusters and Associations: Convection, Rotation, and Dynamos, ASP Conf. Ser., 198, 59
Jameson, R. F., Dobbie, P. D., Hodgkin, S. T., & Pinfield, D. J. 2002, MNRAS, 335, 853
King, I. 1962, AJ, 67, 471
Kroupa, P., Aarseth, S., & Hurley, J. 2001, MNRAS, 321, 699
Luhman, K. L., Rieke, G. H., Lada, C. J., & Lada, E. A. 1998, ApJ, 508, 347
Luhman, K. L., Rieke, G. H., Young, E. T., et al. 2000, ApJ, 540, 1016
Magnier, E., & Cuillandre, J.-C. 2002, PASP, in prep.
Martín, E. L., Basri, G., Gallegos, J. E., et al. 1998, ApJ, 499, L61
Martín, E. L., Brandner, W., Bouvier, J., et al. 2000, ApJ, 543, 299
Moraux, E., Bouvier, J., & Stauffer, J. R. 2001, A&A, 367, 211
Pinfield, D. J., Jameson, R. F., & Hodgkin, S. T. 1998, MNRAS, 299, 955
Pinfield, D. J., Hodgkin, S. T., Jameson, R. F., Cossburn, M. R., & Hambly, N. C. 2000, MNRAS, 313, 347
Reid, N. I., Kirkpatrick, D. J., Liebert, J., et al. 1999, ApJ, 521, 613
Reipurth, B., & Clarke, C. 2001, AJ, 122, 432
Robichon, N., Arenou, F., Mermilliod, J.-C., & Turon, C. 1999, A&A, 345, 471
Simons, D. A., & Becklin, E. E. 1992, ApJ, 390, 431
Stauffer, J. R., Schultz, G., & Kirkpatrick J. D. 1998, ApJ, 499, L199
Stauffer, J. R., Hamilton, D., Probst, R., Rieke, G., & Mateo, M. 1989, ApJ, 344, L21
Stauffer, J. R., Giampapa, M., Liebert, J., & Hamilton, D. 1994, AJ, 108, 160
Stauffer, J. R., Schild, R., Barrado y Navascués, D., et al. 1998, ApJ, 504, 805
Sterzik, M. F., & Durisen, R. H. 1998, A&A, 339, 95
Tej, A., Sahu, K. C., Chandrasekhar, T., & Ashok, N. M. 2002, ApJ, 578, 523
Williams, D. M., Boyle, R. P., Morgan, W. T., et al. 1996, ApJ, 464, 238
Zapatero-Osorio, M. R., Rebolo, R., & Martín, E. L. 1997, A&A, 317, 164
Zapatero-Osorio, M. R., Rebolo, R., Martín, E. L., et al. 1997, ApJ, 491, L81
Zapatero-Osorio, M. R., Rebolo, R., Martín, E. L., et al. 1999, A&AS, 134, 537